Dynamical correlations and a quantum glass phase in a random hopping Bose–Hubbard model

A M Piekarska and T K Kopeć

Institute of Low Temperature and Structure Research, Polish Academy of Sciences, PO Box 1410, 50-950 Wrocław 2, Poland
E-mail: a.piekarska@intibs.pl

Abstract. We investigate a system of interacting bosons with random intersite tunnelling amplitudes. We describe these by introducing Gaussian-distributed hopping integrals into the standard Bose–Hubbard model. This system has been recently shown to exhibit a quantum phase transition to a glassy state. The latter is characterized by a quenched disorder of boson wave-function phases. In this aspect, the system resembles quantum spin-glass systems that attracted much attention. By exploiting this analogy, we employ the well-established methodology originated by Sherrington and Kirkpatrick, which bases on the replica trick and the Trotter–Suzuki expansion. This treatment transforms the original quantum problem into an effective classical one with an additional time-like dimension. Here, we focus on autocorrelation functions of canonical variables of the effective system in the time-like domain. Deep in the disordered phase, we find a highly dynamical nature of correlations in agreement with the expected short memory of the system. This behaviour weakens while approaching and passing the phase boundary, where in the glassy phase asymptotically non-vanishing correlations are encountered. Thus, the state features infinite memory, which is consistent with the quenched nature of glassy disorder with random but frozen boson phases.

Keywords: quantum disordered systems, quantum glasses, correlation functions, Hubbard and related model

Contents

1. Introduction

The interplay of disorder and interactions leads to the emergence of interesting physical phenomena in many-body systems. In particular, quantum effects play an important role in such systems, thus making the phase transition significantly different than it is in the classical case [1]. The rise of quantum simulation techniques [2–4] promises rapid advancement in studies of this kind of systems, as it allows for experimental exploration of arbitrarily formed systems.

Most of the studies concerning disordered bosonic systems was made for the diagonal case [5–7], i.e. when the randomized part of the system is the diagonal matrix element, so in the potential term. It was found [8] that in the presence of such a diagonal disorder, the usual phase transition between superfluid and Mott insulator phases fades, as a new Bose Glass phase emerges between those two. Differently, the off-diagonal case, i.e. the one with randomized tunneling term, is far less explored. Existing works are mostly limited to one-dimensional models [9–11]. As a consequence, it is not yet established whether the direct superfluid to Mott insulator transition is possible in such a setting.

The off-diagonal disorder is a characteristic feature of spin-glass systems. Thus, a bosonic system carrying this ingredient is expected to share at least part of the physical properties with spin glasses. An important difference between diagonal and off-diagonal cases lays in the presence of frustration in the latter [12]. Frustrated systems characterize with multiple degenerate ground states, separated by significantly high potential-energy walls [13]. Thus, at low temperature, the system stays in the vicinity of the initial state in the phase space, and it may never reach the global energy minimum. However, in quantum-mechanical systems this picture changes. This is because quantum effects

can result in broadening of the accessible part of the phase space, as they enable tunnelling between the states even if they are separated by a potential energy barrier [14].

In this paper, we study a system of bosons with quenched off-diagonal disorder. In our previous work [15], we have found the phase transition and characterized the two phases as disordered and glassy. Here, we focus on the dynamic self-interactions, i.e. autocorrelations of canonical variables, and from their behaviour we achieve a better understanding of the time correlations in the system. This allows us to establish that deep in the disordered phase the system is characterized by short memory, while the phase classified as the glassy one corresponds to the quenched disorder. The latter is reflected in asymptotically non-vanishing correlations that may be understood as infinite memory of the system.

2. Methods

2.1. Model

We describe the system under study with the Bose–Hubbard Hamiltonian [8]

$$H = -\sum_{i<j} J_{ij} \left(a_i^\dagger a_j + a_j^\dagger a_i \right) + \frac{U}{2} \sum_i \widehat{n}_i \left(\widehat{n}_i - 1 \right) - \mu \sum_i \widehat{n}_i, \tag{1}$$

where a_i and $a_i^\dagger$ are respectively the annihilation and creation operators for a boson at the site i, while $\widehat{n}_i \equiv a_i^\dagger a_i$ is the particle number operator. The first term of the Hamiltonian describes the random hopping (tunnelling) between each pair of sites, where the amplitudes J_{ij} are identically distributed independent Gaussian random variables with zero mean and the standard deviation equal to $J/\sqrt{N}$. The second and third terms are the standard Bose–Hubbard terms that describe the repulsive on-site interaction (i.e. the energetic penalty for a double occupation) and the chemical potential, respectively. Since the interactions in the considered model are of infinite range, the problem of fluctuations does not arise. On the contrary, fluctuations are an issue in short-range models, however those were found to be very hard to solve in the case of spin glasses, hence we turn into the infinite-range case.

We are about to find the critical lines, defined via the Edwards–Anderson order parameter [16]

$$\mathcal{Q}_{\rm EA} = \frac{1}{N} \sum_i \left\langle |\langle a_i \rangle_{\rm st}|^2 \right\rangle_J, \tag{2}$$

where $\langle \cdots \rangle_J \equiv \prod_{i<j} \int_{-\infty}^{\infty} {\rm d}J_{ij} \cdots \exp[-J_{ij}^2/(2J^2)]$ is the average over the distributions of J_{ij} and $\langle \cdots \rangle_{\rm st} \equiv {\rm Tr} \cdots \exp(-\beta \hat{H})/Z$ is the statistical average, with $Z = {\rm Tr} \exp(-\beta \hat{H})$ being the partition function. However, to make the undertaken derivation convenient and feasible, we need first to write the Hamiltonian in a more suitable basis. For this, we choose the basis of the quasi-momentum $\widehat{P}_i = {\rm i}(a_i^\dagger - a_i)/\sqrt{2}$ and quasi-position $\widehat{Q}_i = (a_i^\dagger + a_i)/\sqrt{2}$ operators, which are defined in the analogy to the standard solution

to the quantum harmonic oscillator problem. Upon this, the Hamiltonian takes the form

$$H = -\sum_{i<j} J_{ij} \left(\widehat{P}_i \widehat{P}_j + \widehat{Q}_i \widehat{Q}_j \right) + \sum_i \left(\widetilde{U} \, \widehat{n}_i^2 - \widetilde{\mu} \, \widehat{n}_i \right), \tag{3}$$

where we have introduced the reduced variables $\widetilde{\mu} = \mu + U/2$ and $\widetilde{U} = U/2$.

2.2. Replica trick and Trotter–Suzuki expansion

We intend to calculate the free energy of the considered system and minimize it. We start by writing the free energy and expanding it using the replica trick [17],

$$F = \frac{1}{\beta} \ln Z = -\lim_{n\to 0} \frac{1}{\beta n} \left(\langle Z^n \rangle_J - 1 \right), \tag{4}$$

where

$$Z^n = \mathrm{Tr} \exp \left(-\beta \sum_{\alpha=1}^n H_\alpha \right), \tag{5}$$

and $\beta = 1/k_B T$. In the last expression, we replicated the Hamiltonian into n copies, each with the same realization of disorder. Next, we split the replicated Hamiltonian into three parts

$$H_{\mathrm{repl}} = \sum_\alpha H_\alpha = H_P + H_Q + H_n, \tag{6}$$

where

$$\begin{aligned}
H_P &= -\sum_\alpha \sum_{i<j} J_{ij} \widehat{P}_{i\alpha} \widehat{P}_{j\alpha}, \\
H_Q &= -\sum_\alpha \sum_{i<j} J_{ij} \widehat{Q}_{i\alpha} \widehat{Q}_{j\alpha}, \\
H_n &= \widetilde{U} \sum_{i\alpha} \widehat{n}_{i\alpha}^2 - \widetilde{\mu} \sum_{i\alpha} \widehat{n}_{i\alpha}.
\end{aligned} \tag{7}$$

These terms do not commute, so we apply the Trotter–Suzuki formula [18] to convert the exponent of the full Hamiltonian into a product of exponents of each of the parts

$$\exp\left(-\beta H_{\mathrm{repl}}\right) \simeq \left[\exp\left(-\frac{\beta}{M} H_P\right) \exp\left(-\frac{\beta}{M} H_Q\right) \exp\left(-\frac{\beta}{M} H_n\right) \right]^M, \tag{8}$$

which converges with rising M and is exact in the limit of $M \to \infty$. In the above, between each pair of consecutive exponents, we insert a summation over a complete set of eigenvectors of either $\widehat{P}$ or $\widehat{Q}$, such that the matrix elements of the first two parts of the Hamiltonian can be calculated. The resulting expression reads

$$Z^n = \text{Tr}_{p,q} \prod_{k=1}^{M} \exp\left[\frac{\beta}{M} \sum_{\alpha} \sum_{i<j} J_{ij} \left(p_{i\alpha}^{(k)} p_{j\alpha}^{(k)} + q_{i\alpha}^{(k)} q_{j\alpha}^{(k)} \right) \right]$$
$$\times \left\langle p^{(k)} \middle| q^{(k)} \right\rangle \left\langle q^{(k)} \middle| \exp\left(-\frac{\beta H_n}{M} \right) \middle| p^{(k+1)} \right\rangle, \tag{9}$$

where the trace runs over all configurations of $\{p_{i\alpha}^{(k)}; q_{i\alpha}^{(k)}\}$, i.e.

$$\text{Tr}_{p,q}(\cdot) \equiv \sum_{p_{11}^{(1)}} \cdots \sum_{p_{Nn}^{(M)}} \sum_{q_{11}^{(1)}} \cdots \sum_{q_{Nn}^{(M)}} (\cdot), \tag{10}$$

and we have introduced product states $|p^{(k)}\rangle = \bigotimes_{i,\alpha} |p_{i\alpha}^{(k)}\rangle$, while variables $p_{i\alpha}^{(k)}$ are the eigenvalues of the operator $\widehat{P}_{i\alpha}$, i.e. $\widehat{P}_{i\alpha}|p_{i\alpha}^{(k)}\rangle = p_{i\alpha}^{(k)}|p_{i\alpha}^{(k)}\rangle$, and $q_{i\alpha}^{(k)}$ are the eigenvalues of $\widehat{Q}_{i\alpha}$. Different J_{ij}s may be now treated separately and therefore we can perform the averaging over Gaussian distributions, which results in the following expression

$$\langle Z^n \rangle = \text{Tr}_{pq} \mathcal{M}_{p,q} \prod_{i<j} \exp\left[\frac{J^2\beta^2}{2M^2N} \left(\sum_{k\alpha} \left(p_{i\alpha}^{(k)} p_{j\alpha}^{(k)} + q_{i\alpha}^{(k)} q_{j\alpha}^{(k)} \right) \right)^2 \right], \tag{11}$$

where $\mathcal{M}_{pq}$ is a product of matrix elements

$$\mathcal{M}_{p,q} = \prod_{i} \mathcal{M}_{p,q}^{(i)} = \prod_{i,\alpha} \prod_{k} \left\langle p_{i\alpha}^{(k)} \middle| q_{i\alpha}^{(k)} \right\rangle \left\langle q_{i\alpha}^{(k)} \middle| \exp\left(-\frac{\beta H_n}{M} \right) \middle| p_{i\alpha}^{(k+1)} \right\rangle \tag{12}$$

that will not be analytically handled in this derivation.

At this point, the expression for $\langle Z^n \rangle$ becomes classical. The only reminiscence of the quantum nature of the system is implicitly present in $\mathcal{M}_{pq}$. However, we can treat it as an unknown function of variables $p_{i\alpha}^{(k)}, p_{i\alpha}^{(k)}$, thus effectively making it classical. This means that we have mapped a quantum-mechanical problem onto a classical one, but with an additional time-like dimension.

2.3. Self-consistent solution

We apply the Hubbard–Stratonovich transformation to the terms containing four variables and two sites, which results in reducing the problem to just a single site and introduction of three sets of order parameters labelled $\lambda_{k\alpha k'\alpha'}^{P}$, $\lambda_{k\alpha k'\alpha'}^{Q}$, and $\lambda_{k\alpha k'\alpha'}^{PQ}$:

$$\langle Z^n \rangle = \text{Tr}_{pq} \mathcal{M}_{p,q} \prod_{k\alpha k'\alpha'} \exp\left[-\frac{J^2\beta^2}{4M^2N} \sum_{i} \left((p_{i\alpha}^{(k)})^2 + (q_{i\alpha}^{(k)})^2 \right) \left((p_{i\alpha'}^{(k')})^2 + (q_{i\alpha'}^{(k')})^2 \right) \right]$$
$$\times \left[\sqrt{\frac{N}{\pi}} \int d\lambda_{k\alpha k'\alpha'}^{P} \exp\left(-N(\lambda_{k\alpha k'\alpha'}^{P})^2 + \frac{\lambda_{k\alpha k'\alpha'}^{P} J\beta}{M} \sum_{i} p_{i\alpha}^{(k)} p_{i\alpha'}^{(k')} \right) \right]$$
$$\times \left[\sqrt{\frac{N}{\pi}} \int d\lambda_{k\alpha k'\alpha'}^{Q} \exp\left(-N(\lambda_{k\alpha k'\alpha'}^{Q})^2 + \frac{\lambda_{k\alpha k'\alpha'}^{Q} J\beta}{M} \sum_{i} q_{i\alpha}^{(k)} q_{i\alpha'}^{(k')} \right) \right]$$
$$\times \left[\sqrt{\frac{N}{2\pi}} \int d\lambda_{k\alpha k'\alpha'}^{PQ} \exp\left(-\frac{N(\lambda_{k\alpha k'\alpha'}^{PQ})^2}{2} + \frac{\lambda_{k\alpha k'\alpha'}^{PQ} J\beta}{M} \sum_{i} p_{i\alpha}^{(k)} q_{i\alpha'}^{(k')} \right) \right]$$

$$\propto \mathrm{Tr}_{pq} \int\!\!\int \ldots \int \left(\prod_{k\alpha k'\alpha'} \mathrm{d}\lambda^P_{k\alpha k'\alpha'} \mathrm{d}\lambda^Q_{k\alpha k'\alpha'} \mathrm{d}\lambda^{PQ}_{k\alpha k'\alpha'} \right)$$

$$\times \left\{ \prod_{k\alpha k'\alpha'} \exp\left[-N(\lambda^P_{k\alpha k'\alpha'})^2 - N(\lambda^P_{k\alpha k'\alpha'})^2 - \frac{N(\lambda^{PQ}_{k\alpha k'\alpha'})^2}{2} \right] \right\}$$

$$\times \prod_i \mathcal{M}^{(i)}_{p,q} \left\{ \prod_{k\alpha k'\alpha'} \exp\left[-\frac{J^2\beta^2}{4M^2N} \left((p^{(k)}_{i\alpha})^2 + (q^{(k)}_{i\alpha})^2 \right) \left((p^{(k')}_{i\alpha'})^2 + (q^{(k')}_{i\alpha'})^2 \right) \right] \right.$$

$$\left. \times \exp\left[\frac{\lambda^P_{k\alpha k'\alpha'} J\beta}{M} p^{(k)}_{i\alpha} p^{(k')}_{i\alpha'} + \frac{\lambda^Q_{k\alpha k'\alpha'} J\beta}{M} q^{(k)}_{i\alpha} q^{(k')}_{i\alpha'} + \frac{\lambda^{PQ}_{k\alpha k'\alpha'} J\beta}{M} p^{(k)}_{i\alpha} q^{(k')}_{i\alpha'} \right] \right\}. \quad (13)$$

After carrying out the summation over i, we can rewrite the above expression in the form

$$\langle Z^n \rangle \propto \int\!\!\int \ldots \int \left(\prod_{k\alpha k'\alpha'} \mathrm{d}\lambda^P_{k\alpha k'\alpha'} \mathrm{d}\lambda^Q_{k\alpha k'\alpha'} \mathrm{d}\lambda^{PQ}_{k\alpha k'\alpha'} \right)$$

$$\times \exp\left[-N\mathcal{F}\left(\{\lambda^P_{k\alpha k'\alpha'} \lambda^Q_{k\alpha k'\alpha'}, \lambda^{PQ}_{k\alpha k'\alpha'}\} \right) \right], \quad (14)$$

where we have defined the effective free energy

$$\mathcal{F} = \sum_{k\alpha k'\alpha'} \left[(\lambda^P_{k\alpha k'\alpha'})^2 + (\lambda^Q_{k\alpha k'\alpha'})^2 + \frac{(\lambda^{PQ}_{k\alpha k'\alpha'})^2}{2} \right] - \ln \mathrm{Tr}_{pq} \exp\left(-\beta H_{\mathrm{eff}} \right), \quad (15)$$

and the effective Hamiltonian

$$-\beta H_{\mathrm{eff}} = -\frac{1}{N} \left[\sum_{k\alpha} \frac{J\beta}{2M} \left((p^{(k)}_\alpha)^2 + (q^{(k)}_\alpha)^2 \right) \right]^2 + \ln \mathcal{M}_{pq}$$

$$+ \frac{J\beta}{M} \sum_{k\alpha k'\alpha'} \left[\lambda^P_{k\alpha k'\alpha'} p^{(k)}_\alpha p^{(k')}_{\alpha'} + \lambda^Q_{k\alpha k'\alpha'} q^{(k)}_\alpha q^{(k')}_{\alpha'} + \lambda^{PQ}_{k\alpha k'\alpha'} p^{(k)}_\alpha q^{(k')}_{\alpha'} \right]. \quad (16)$$

In the thermodynamic limit, the first term of this Hamiltonian vanishes, while the saddle-point method gives the minimum of $\langle Z^n \rangle$ at $\partial\mathcal{F}/\partial x = 0$ for all $x \in \{\lambda^X_{k\alpha k'\alpha'}\}$ $(X = P, Q, PQ)$, resulting in the following expressions for order parameters:

$$\lambda^P_{k\alpha k'\alpha'} = \frac{J\beta}{2M} \left\langle p^{(k)}_\alpha p^{(k')}_{\alpha'} \right\rangle_{\mathrm{eff}},$$

$$\lambda^Q_{k\alpha k'\alpha'} = \frac{J\beta}{2M} \left\langle q^{(k)}_\alpha q^{(k')}_{\alpha'} \right\rangle_{\mathrm{eff}}, \quad (17)$$

$$\lambda^{PQ}_{k\alpha k'\alpha'} = \frac{J\beta}{M} \left\langle p^{(k)}_\alpha q^{(k')}_{\alpha'} \right\rangle_{\mathrm{eff}},$$

where $\langle \cdots \rangle_{\mathrm{eff}}$ are the thermodynamical averages taken with the Hamiltonian H_{eff} and defined as

$$\langle X \rangle_{\mathrm{eff}} = \frac{\mathrm{Tr}_{pq} X \exp\left(-\beta H_{\mathrm{eff}} \right)}{\mathrm{Tr}_{pq} \exp\left(-\beta H_{\mathrm{eff}} \right)}. \quad (18)$$

Note, that besides the explicit dependence of $\lambda_{k\alpha k'\alpha'}^{X}$ on $p_\alpha^{(k)}$, and thus on the Trotter index k, there is also an implicit dependence via the averaging, as H_{eff} is a function of $\{p_{i\alpha}^{(k)}; q_{i\alpha}^{(k)}\}$, and that this dependence is not necessarily symmetric on swapping indices. In the limit of $M \to \infty$, the discrete indices k transform into a continuous variable. Such a description has been used in systems that were possible to be fully investigated analytically [14]. Here, we are forced to resort to numerical solutions. Due to the symmetries in the Hamiltonian, we have

$$\left\langle p_\alpha^{(k)} p_{\alpha'}^{(k')} \right\rangle_{\mathrm{eff}} = \left\langle q_\alpha^{(k)} q_{\alpha'}^{(k')} \right\rangle_{\mathrm{eff}}, \qquad \left\langle p_\alpha^{(k)} q_{\alpha'}^{(k')} \right\rangle_{\mathrm{eff}} = 0, \tag{19}$$

meaning there is just one unique set of variables $\lambda_{k\alpha k'\alpha'}^{P} = \lambda_{k\alpha k'\alpha'}^{Q} \equiv \lambda_{k\alpha k'\alpha'}$.

2.4. Dynamic self-interactions

These order-parameter variables introduced above are of two types with regard to the replica space:

$$\lambda_{k\alpha k'\alpha'} = \delta_{\alpha\alpha'} \mathcal{R}_{kk'} + (1 - \delta_{\alpha\alpha'}) \mathcal{Q}_{\alpha\alpha'}. \tag{20}$$

In the above, the variables denoted by $\mathcal{Q}_{\alpha\alpha'}$, acting in two different replica subspaces ($\alpha \neq \alpha'$), are static (not dependent on k) and related to the Edwards–Anderson order parameter (2)

$$\mathcal{Q}_{\mathrm{EA}} = \lim_{n \to 0} \frac{2}{n(n-1)} \sum_{\alpha > \alpha'} \mathcal{Q}_{\alpha\alpha'}. \tag{21}$$

On the other hand, those acting in a common replica subspace ($\alpha = \alpha'$) are called dynamic self-interactions. They are denoted by $\mathcal{R}_{kk'}$ and they depend on the absolute difference of indices $|k - k'|$ only. Since the Trotter index k has a character of a time axis, the self-interactions serve as a measure of the memory of the system.

After inserting the decomposition (20) into equations (15) and (16), the effective free energy and Hamiltonian now read respectively

$$\mathcal{F} = 2n \sum_{kk'} \mathcal{R}_{kk'}^2 + 2M^2 \sum_{\alpha \neq \alpha'} \mathcal{Q}_{\alpha\alpha'}^2 - \ln \mathrm{Tr}_{pq} \exp\left(-\beta H_{\mathrm{eff}}\right) \tag{22}$$

and

$$-\beta H_{\mathrm{eff}} = \frac{J\beta}{M} \sum_{k\alpha k'\alpha'} [\delta_{\alpha\alpha'} \mathcal{R}_{kk'} + (1 - \delta_{\alpha\alpha'}) \mathcal{Q}_{\alpha\alpha'}] \left(p_\alpha^{(k)} p_{\alpha'}^{(k')} + q_\alpha^{(k)} q_{\alpha'}^{(k')}\right) + \ln \mathcal{M}_{pq}. \tag{23}$$

We are working within the replica-symmetric case and put $\mathcal{Q}_{\alpha\alpha'} = 0$. The replicas decouple now, and we can perform the summation over α as well as the limit of $n \to 0$. The effective free energy and Hamiltonian take their final forms

$$\mathcal{F} = 2 \sum_{kk'} \mathcal{R}_{kk'}^2 - \ln \mathrm{Tr}_{pq} \exp\left(-\beta H_{\mathrm{eff}}\right) \tag{24}$$

and

$$-\beta H_{\text{eff}} = \frac{J\beta}{M} \sum_{kk'} \mathcal{R}_{kk'} \left(p_k p_{k'} + q_k q_{k'} \right) + \ln \mathcal{M}_{pq} \tag{25}$$

where we have moved k to the subscript for simplicity. The self-consistent equation reads now

$$\mathcal{R}_{kk'} = \frac{J\beta}{2M} \langle p_k p_{k'} \rangle_{\text{eff}}. \tag{26}$$

To obtain the critical line, we expand the free energy (22) to the second order in the spin-glass order parameter $\mathcal{Q}_{\alpha\alpha'}$, and following the Landau theory we arrive at the condition

$$\sum_k \mathcal{R}_{kk'} = \frac{1}{2}, \tag{27}$$

which corresponds to the point where the Edwards–Anderson order parameter $\mathcal{Q}_{\text{EA}}$ reveals the phase transition. The cases of $\sum_k \mathcal{R}_{kk'} < \frac{1}{2}$ and $\sum_k \mathcal{R}_{kk'} > \frac{1}{2}$ correspond to the disordered ($\mathcal{Q}_{\text{EA}} = 0$) and the glassy ($\mathcal{Q}_{\text{EA}} \neq 0$) phase, respectively.

2.5. Numerical calculations

To obtain quantitative results, we solve the self-consistent equations (26) numerically. These contain a summation over full bases of the operators $\widehat{P}$ and $\widehat{Q}$, which are infinite and therefore cannot be numerically calculated. To circumvent this, we truncate the Hilbert space to contain only the states with up to two particles per site, making the trace finite. The probability of adding two particles via thermal excitation to a site initially containing n particles is given by

$$\exp\left[\frac{\frac{U}{2}n(n-1) - \mu n}{T} - \frac{\frac{U}{2}(n+2)(n+1) - \mu(n+2)}{T} \right] = \exp\left(\frac{2\mu/U - (2n+1)}{T/U} \right), \tag{28}$$

which becomes $\exp(-U/T)$ for $\mu/U = n$ and lower for $\mu/U < n$. At temperatures considered here, $T/U \in \{0.01, 0.05, 0.1\}$, these values are $\exp(-U/T) = 3.7 \cdot 10^{-44}$, $2.1 \cdot 10^{-9}$, $4.5 \cdot 10^{-5}$, respectively. Therefore, we consider two-particle excitation extremely unlikely for $\mu/U \leqslant n \leqslant 1$ and assume the physical properties of the system with $\mu/U \leqslant 1$ to be correctly estimated within a description employing up to two particles per site. However, the number of terms in the summation is still as high as 9^M, so it remains the main challenge of the numerical calculation and significantly limits the highest available M, as the Quantum Monte Carlo method is not available in this case due to a severe sign problem [19].

The self-consistent calculation is performed in the following manner. First, we fix the parameters M, μ/U, J/U and T/U and choose the initial values of $\mathcal{R}_{kk'}$ (it is computationally beneficial to use the result of a previous computation in a series with varying parameter). Then, we keep replacing the values of $\mathcal{R}_{kk'}$ with the result of the right-hand side of equation (26), in which the previous set of $\mathcal{R}_{kk'}$ was used in the averaging. We stop the computation when the relative change in $\mathcal{R}_{kk'}$ is below a given threshold. In

order to find the critical line, we apply the binary search algorithm along the J/U axis while keeping the other parameters constant.

To handle the term $\mathcal{M}_{pq}$, we precompute overlaps of the form $\langle p|q \rangle$ and matrix elements of the form $\left\langle q \left| \exp\left(\frac{\beta\tilde{\mu}}{M}\hat{n} - \frac{\beta\tilde{U}}{M}\hat{n}^2\right) \right| p \right\rangle$ by exact diagonalization of the operators $\widehat{P}$, $\widehat{Q}$ and $\exp\left(\frac{\beta\tilde{\mu}}{M}\hat{n} - \frac{\beta\tilde{U}}{M}\hat{n}^2\right)$ in the truncated basis. This enables fast calculation of $\mathcal{M}_{pq}$ by looking up the values for each of the processed pairs $p^{(k)}, q^{(k)}$ (for the overlap) or $q^{(k)}, p^{(k+1)}$ (for the matrix element).

3. Results

First, we find the phase diagram of the system at three various temperatures, and we plot it in figure 1. The critical line is found in the space spanned by Hamiltonian parameters: chemical potential μ and standard deviation of the intersite interaction J normalized by U. Below the phase transition line, i.e. at lower values of J/U, we find a disordered phase, while above the line the glassy phase is present. We are working with a finite value of $M = 10$, but based on comparison with the $M = 8$ case as well as on our previous work [15], we expect that the $T/U = 0.05$ and $T/U = 0.1$ lines are close to the $M \to \infty$ extrapolation, while the $T/U = 0.01$ one is less accurate but remains a good approximation of the converged result. Therefore, we will present part of the results for all three temperature choices, but will focus only on the $T/U = 0.05$ case for a more detailed study.

We cut the phase diagram along the vertical line at $\mu/U = 0.4$ (marked in figure 1 with a dotted line) and plot the corresponding dynamic self-interactions $\mathcal{R}_{|k-k'|}$ in figure 2. To comply with the standard definition of the correlation function, we analyse the normalized self-interactions $\widetilde{\mathcal{R}}_{|k-k'|} \equiv \mathcal{R}_{|k-k'|}/\mathcal{R}_0$. The figure is split into three panels corresponding to chosen temperatures. Each line in the plots corresponds to a single value of J/U, with the colour and line style indicating in which phase the system is for that value of J/U. Since we are working in the approximation with $\mathcal{Q}_{\mathrm{EA}} = 0$, we consider the results in the disordered phase valid, while in the glassy phase their reliability decreases with the distance from the phase transition. Even though we are not considering the glassy phase within the full description of the Edwards–Anderson order parameter, our handling should be sufficient to probe the physical properties close to the critical line. From our calculations it can be seen that in the glassy phase the self-correlations saturate. This means that even for large time differences there are correlations, so the system exhibits long-term memory. On the other hand, in the disordered phase the correlations decline monotonically, meaning the system quickly loses the dependence on the initial state. This distinction becomes stronger with decreasing temperature. In the limit of $M \to \infty$, the value of $\widetilde{\mathcal{R}}_{M/2}$ becomes the infinite-time correlation, and we will denote it by $\widetilde{\mathcal{R}}_\infty$. Working in finite M, we are using $\widetilde{\mathcal{R}}_{M/2}$ as an approximation of this value.

Noting the monotonic nature of $\widetilde{\mathcal{R}}_{|k-k'|}$, we consider the value $\widetilde{\mathcal{R}}_{M/2}$ as containing nearly full information on the decay of correlations. Stated this, we plot a colour map of its values for $M = 10$ in figure 3 as a function of the same variables (μ/U and
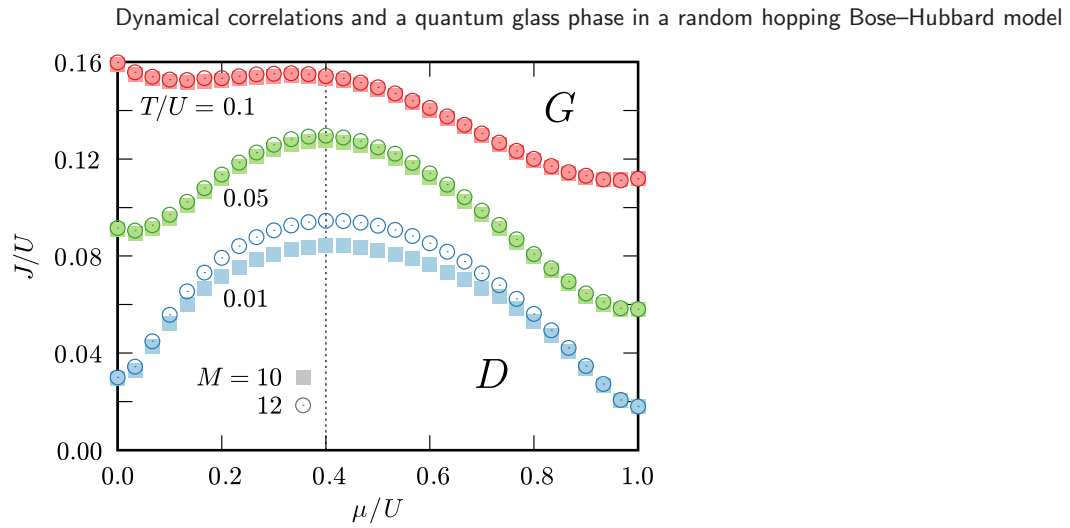
Figure 1. The phase diagram of the system at three chosen temperatures and for two values of M (marked in the plot). Labels D and G stand for the disordered and the glassy phase, respectively.
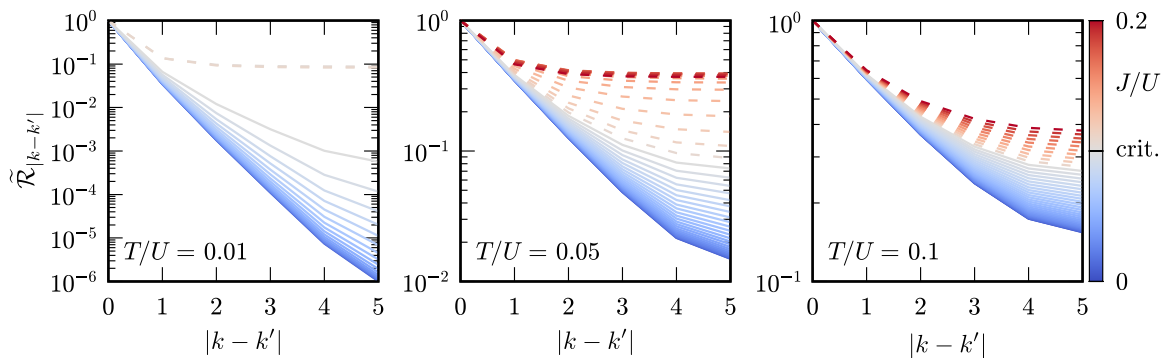

Figure 2. Normalized dynamic self-interactions $\widetilde{\mathcal{R}}_{|k-k'|}$ as a function of $|k-k'|$ calculated along the vertical cut marked in figure 1 at three chosen temperature values (panels). The lines corresponding to J/U in the disordered phase are solid and drawn with a gradient of blue colours, while those corresponding to J/U in the glassy regime are dashed and drawn with a red hue. Note that the critical value of J/U varies between the panels. The data is drawn with lines for visibility.

J/U) as the phase diagram presented above in figure 1. We notice that the decline is the steepest deep in the disordered phase, while the correlation time increases when going towards the glassy phase or integer chemical-potential values. The latter can be explained by the fact, that at zero temperature the glassy phase is present all the way down to $J/U = 0$ in the integer chemical-potential values, while at fractional values of μ/U the glassy-phase threshold is finite [15].

We also choose to cut the $T/U = 0.05$ phase diagram along $J/U = 0.04$ and $J/U = 0.12$ (as marked in figure 3 with the dotted lines) and plot the corresponding dynamical self-interactions versus μ/U in figure 4. Here, the saturation around integer μ/U that has been mentioned before is even more visible. We can also compare the two J/U choices in absolute terms: the zero-time self interactions are of the same order in both cases, and it is the long-time behavior that differs and makes it possible to distinguish the short- and long-memory nature of studied phases.
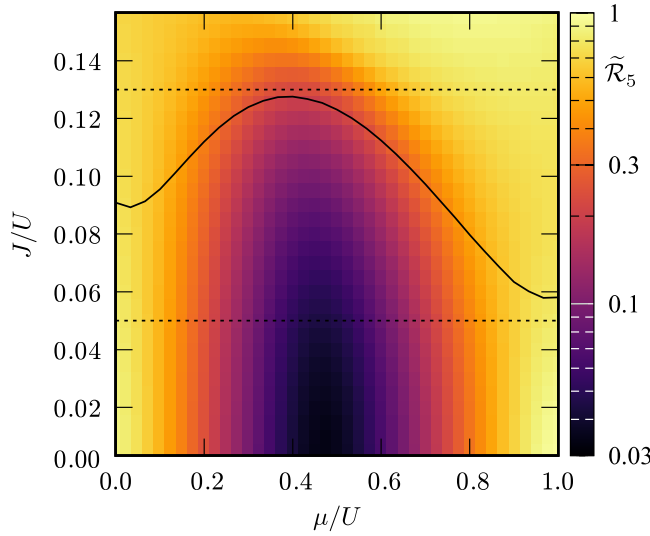
Figure 3. A heatmap showing values of $\widetilde{\mathcal{R}}_5$ for the full considered range of μ/U and J/U, calculated at $T/U = 0.05$ and for $M = 10$. The solid line marks the phase transition.
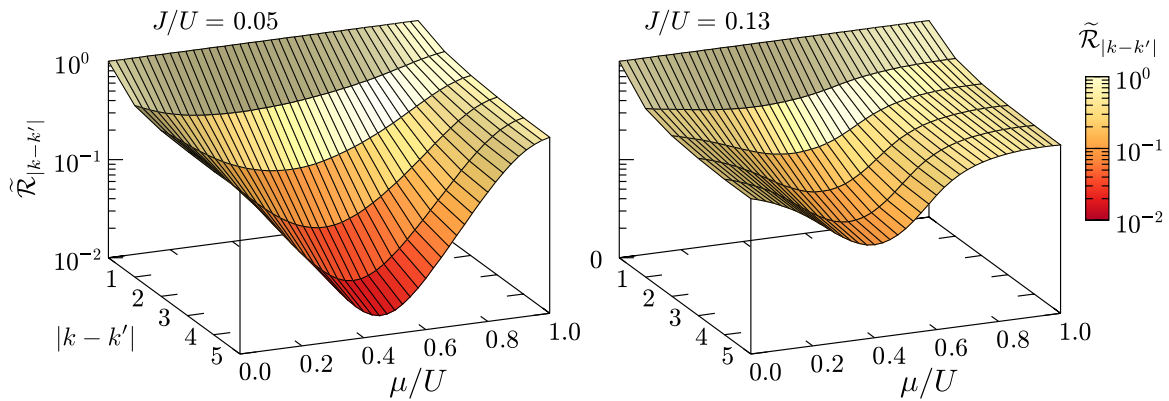

Figure 4. Normalized dynamic self-interactions $\widetilde{\mathcal{R}}_{|k-k'|}$ as a function of $|k - k'|$ calculated along the two horizontal cuts marked in figure 3 and at $T/U = 0.05$. Note the common z axis for both panels.

To minimize the effect of the finite value of M on the observed quantities, we extrapolate the values of $\widetilde{\mathcal{R}}_{M/2}$ to $M \to \infty$ and plot the estimated $\widetilde{\mathcal{R}}_\infty$ as a function of J/U in figure 5 for a selection of temperatures near the earlier discussed $T/U = 0.05$. The phase transition point varies between distinct values of T/U and M but in majority of the cases it takes place in the shaded area. We find that in the disordered phase decreasing temperature results in weaker infinite-time correlations, while towards the glassy phase this dependence gets reversed. Note, that due to $\mathcal{Q}_{\mathrm{EA}} = 0$, the calculations become less and less accurate deeper in the glassy phase. The extrapolated values of $\widetilde{\mathcal{R}}_\infty$ origin from fitting the expected dependence of the form $c + a\,(b + M^2)^{-1}$ [20] to the values of $\widetilde{\mathcal{R}}_{M/2}$ in the range of $M \in [4, 12]$. We show examples of such fits in figure 6(a).

In the disordered phase, the dependence of $\widetilde{\mathcal{R}}_\infty$ on J/U turns out exponential, therefore we fit it and extract the $J/U \to 0$ values. We plot them as a function of temperature
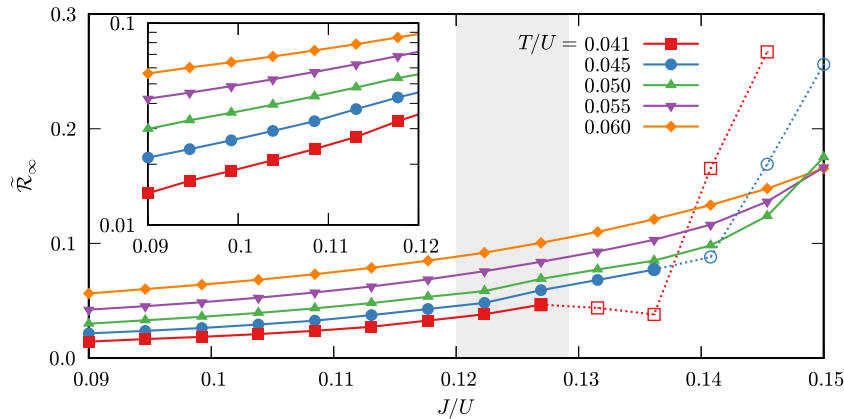
Figure 5. Normalized infinite-time correlations $\widetilde{\mathcal{R}}_\infty$ as a function of J/U at selected temperatures. The points drawn with open symbols and connected by dotted lines correspond to less reliable fits. The shaded area marks the phase transition. The inset shows a logarithmic-scale zoom on the low J/U part of the same curves. The lines are to guide the eye only.
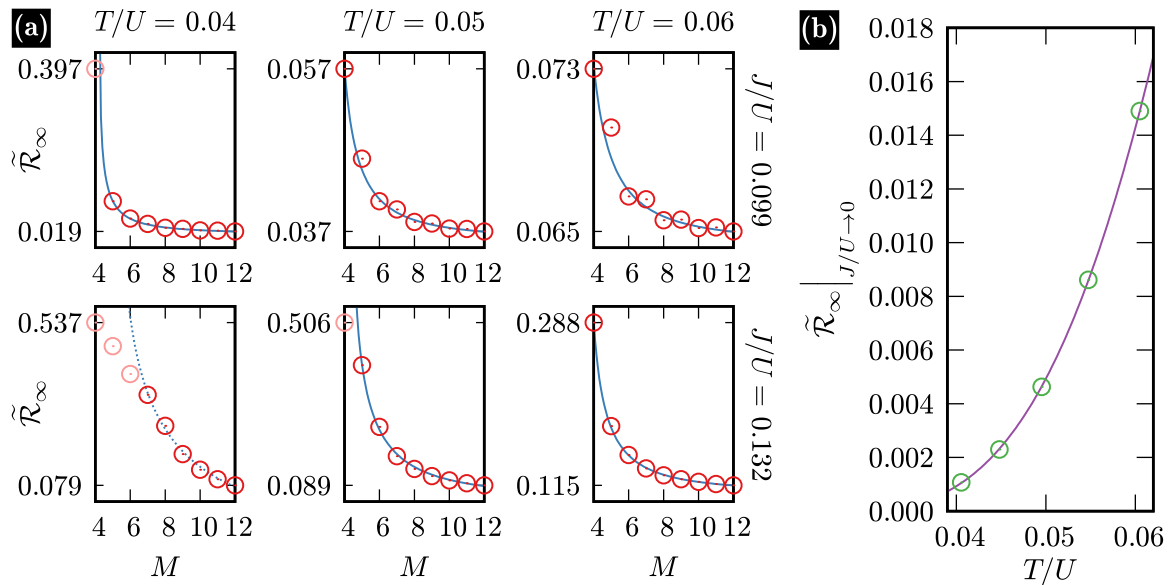

Figure 6. (a) Exemplary fits of the M-dependence of the normalized infinite-time correlations $\widetilde{\mathcal{R}}_\infty$. Columns correspond to varying T/U, while rows present two distinct values of J/U. Data is presented with points, while the lines are fits. The lightened data points were not taken into account while fitting. The fit drawn with a dotted line (at $T/U = 0.04$ and $J/U = 0.132$) is an example of a one marked as less reliable in figure 5. (b) The $J/U \to 0$ behaviour of the normalized infinite-time correlation $\widetilde{\mathcal{R}}_\infty$. Data is presented with points, while the fit is drawn with a line.

in figure 6(b). We notice that $\widetilde{\mathcal{R}}_\infty\big|_{J/U \to 0}(T/U)$ has the form of $c + a\exp(-bU/T)$, with the variable c negligibly small. Thus, we conclude that $\widetilde{\mathcal{R}}_\infty\big|_{J/U \to 0}$ vanishes at $T/U \to 0$, meaning that there are no infinite-time correlations at $T/U = 0$ and $J/U = 0$, which is in line with the expectations for the disordered phase.

4. Summary

We have studied dynamic self-interactions in a system of interacting bosons with off-diagonal disorder. Following the theoretical framework proven to be successful in spin glasses, we have found and characterized the phases. Studying their properties, we have established that deep in the disordered phase the correlations fade quickly. This behavior is most pronounced at low temperatures and for half-integer chemical potentials. Towards the glassy phase, the correlation time increases, and above the critical line self-interactions become asymptotically non-vanishing. This is in line with the expectation that contrarily to the disordered phase which loses the dependence on the initial state quickly, the glassy phase has long-term memory, which is one of the features making the glassy states interesting. The low-temperature phase is, however, not accurately described within the used approximation of $\mathcal{Q}_{EA} = 0$. To study it thoroughly, one would need to allow $\mathcal{Q}_{EA}$ to become nonzero. Additionally, extending the analysis to the replica-symmetry broken case [21] might be needed as well, as has been the case in quantum spin-glass systems [22].

Acknowledgments

References

[1] Sachdev S 1999 *Quantum Phase Transitions* (Cambridge: Cambridge University Press)
[2] Jaksch D and Zoller P 2005 *Ann. Phys.* **315** 52–79
[3] Blatt R and Roos C F 2012 *Nat. Phys.* **8** 277–84
[4] Feynman R P 1982 *Int. J. Theor. Phys.* **21** 467–88
[5] Gimperlein H, Wessel S, Schmiedmayer J and Santos L 2005 *Phys. Rev. Lett.* **95** 170401
[6] Fallani L, Lye J E, Guarrera V, Fort C and Inguscio M 2007 *Phys. Rev. Lett.* **98** 130404
[7] Singh K G and Rokhsar D S 1992 *Phys. Rev.* B **46** 3002–8
[8] Fisher M P A, Weichman P B, Grinstein G and Fisher D S 1989 *Phys. Rev.* B **40** 546–70
[9] Prokof'ev N and Svistunov B 2004 *Phys. Rev. Lett.* **92** 015703
[10] Balabanyan K G, Prokof'ev N and Svistunov B 2005 *Phys. Rev. Lett.* **95** 055701
[11] Sengupta P and Haas S 2007 *Phys. Rev. Lett.* **99** 050403
[12] Fradkin E, Huberman B A and Shenker S H 1978 *Phys. Rev.* B **18** 4789–814
[13] Nemoto K 1988 *J. Phys. A: Math. Gen.* **21** L287–94
[14] Bray A J and Moore M A 1980 *J. Phys. C: Solid State Phys.* **13** L655–60
[15] Piekarska A and Kopeć T 2018 *Phys. Rev. Lett.* **120** 160401
[16] Edwards S F and Anderson P W 1975 *J. Phys.* F **5** 965
[17] Sherrington D and Kirkpatrick S 1975 *Phys. Rev. Lett.* **35** 1792–6
[18] Trotter H F 1959 *Proc. Am. Math. Soc.* **10** 545
[19] Piekarska A and Kopeć T 2019 *Acta Phys. Pol.* A **135** 78–81
[20] Suzuki M 1985 *Phys. Lett.* A **113** 299–300
[21] Parisi G 1980 *J. Phys. A: Math. Gen.* **13** L115–21
[22] Büttner G and Usadel K D 1990 *Phys. Rev.* B **41** 428–31